

231120

UCRL-JC-126732

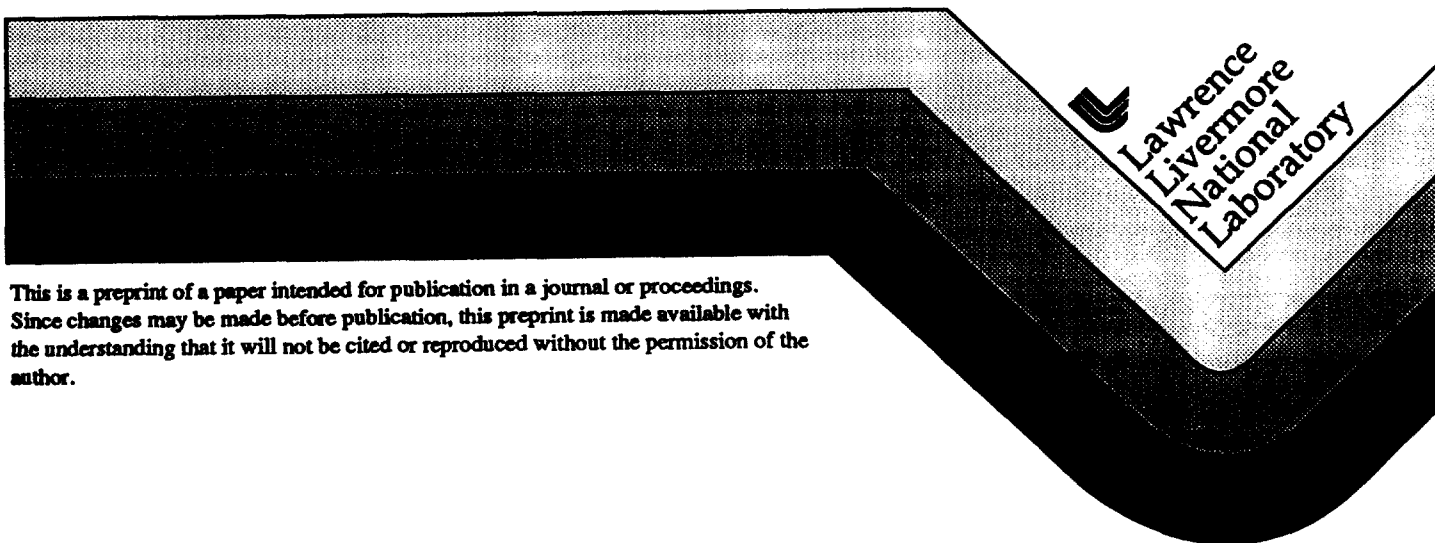
PREPRINT

**Lawrence Livermore National Laboratory's  
PEREGRINE Project**

C. L. Hartmann Siantar, P. M. Bergstrom, W. P. Chandler, L. Chase,  
L. J. Cox, T. P. Daly, D. Garrett, S. M. Hornstein, R. K. House,  
E. I. Moses, R. W. Patterson, J. A. Rathkopf, A. Schach von Wittenau

This paper was prepared for submittal to the  
12th International Conference on the Use of Computers in Radiation Therapy  
Salt Lake City, UT  
May 27-30, 1997

March 1, 1997



#### DISCLAIMER

This document was prepared as an account of work sponsored by an agency of the United States Government. Neither the United States Government nor the University of California nor any of their employees, makes any warranty, express or implied, or assumes any legal liability or responsibility for the accuracy, completeness, or usefulness of any information, apparatus, product, or process disclosed, or represents that its use would not infringe privately owned rights. Reference herein to any specific commercial products, process, or service by trade name, trademark, manufacturer, or otherwise, does not necessarily constitute or imply its endorsement, recommendation, or favoring by the United States Government or the University of California. The views and opinions of authors expressed herein do not necessarily state or reflect those of the United States Government or the University of California, and shall not be used for advertising or product endorsement purposes.

# Lawrence Livermore National Laboratory's PEREGRINE Project\*

Christine L. Hartmann Siantar, Paul M. Bergstrom, William P. Chandler, Lila Chase, Lawrence J. Cox, Thomas P. Daly, Dewey Garrett, Steven M. Hornstein, Ronald K. House, Edward I. Moses, Ralph W. Patterson, James A. Rathkopf and Alexis Schach von Wittenau  
Lawrence Livermore National Laboratory, Livermore, CA

## INTRODUCTION

PEREGRINE is an all-particle, first-principles 3D Monte Carlo dose calculation system designed to serve as a dose calculation engine for clinical radiation therapy treatment planning (RTP) systems.

By taking advantage of recent advances in low-cost computer commodity hardware, modern symmetric multiprocessor architectures and state-of-the-art Monte Carlo transport algorithms, PEREGRINE performs high-resolution, high accuracy, Monte Carlo RTP calculations in times that are reasonable for clinical use. Because of its speed and simple interface with conventional treatment planning systems, PEREGRINE brings Monte Carlo radiation transport calculations to the clinical RTP desktop environment.

Although PEREGRINE is designed to calculate dose distributions for photon, electron, fast neutron and proton therapy, this paper focuses on photon teletherapy.

## IMPLEMENTATION OF MONTE CARLO FOR RADIATION THERAPY DOSE CALCULATIONS

The PEREGRINE Monte Carlo dose calculation process depends on four key elements: complete material composition description of the patient as a transport mesh, accurate characterization of the radiation source, first-principles particle transport algorithms, and reliable, self-consistent particle-interaction databases. PEREGRINE uses these elements to provide efficient, accurate Monte Carlo transport calculation for radiation therapy planning.

### Patient Description

The patient transport mesh is a Cartesian map of material composition and density determined from the patient's CT scan. Each CT scan pixel is used to identify the atomic composition and density of a corresponding transport mesh voxel. Atomic composition is determined from CT threshold values set by the user or by default values based on user-specified CT numbers for air and water. The user also assigns materials and densities to the interior of contoured structures.

If the user specifies a structure as the outer contour of the patient, PEREGRINE constructs a transport mesh that is limited to the maximum extent of that structure, and sets all voxels outside that structure to be air. This provides a simple method of subtracting the CT table from the calculation.

The default resolution of the transport mesh is  $1 \times 1 \times 3$  mm, for small-volume areas such as the head and neck, or  $2 \times 2 \times 10$  mm, for large-volume treatment sites such as the chest and pelvis. The resolution can also be reduced from the CT scan resolution. For reduced-resolution voxels, material composition and density are determined as the average of all CT pixels that fall within the transport mesh voxel.

### Radiation Source Description

The PEREGRINE source model [1], designed to provide an compact, accurate representation of the radiation source, divides the beam-delivery system into two parts: an accelerator-specific upper portion and a treatment-specific lower part.

The accelerator-specific upper portion, consisting of the electron target, flattening filter, primary collimator and monitor chamber is precharacterized based on the machine vendor's model-specific information. These precharacterized sources are derived from Monte Carlo simulations from off-line Monte Carlo simulations using BEAM [2] and MCNP4A [3]. Particle histories from off-line simulations are cast into multidimensional probability distributions, which are sampled during the PEREGRINE calculation [2]. The photon beam is divided into three subsources: primary, scattered, and contaminant. Separating the source into subsources facilitates investigation of the contributions of each individual component. To ensure site-specific model accuracy, the installation procedures will consist of a limited number of beam description parameter adjustments, based on simple beam characterization measurements.

The lower portion of the radiation source consists of treatment-specific beam modifiers such as collimators, apertures, blocks, and wedges. This portion is modeled explicitly during each PEREGRINE calculation. Particles are transported through this portion of the source using a pared-down transport scheme. Photons intersecting the collimator jaws are absorbed. Photons intersecting the block or wedge are tracked through the material using the same physical database and methods described below for patient transport. However, all electrons set in motion by photon interactions in the block or wedge are immediately absorbed. The validity of these assumptions is discussed in [1] and [4].

### Monte Carlo Transport Methods

Using the Monte Carlo transport method, PEREGRINE tracks all photons, electrons, positrons and their daughter products through the transport mesh until they reach a specified minimum tracking energy or leave the patient transport mesh. Developing good statistics requires tracking millions of representative particles (histories) through the patient transport mesh. During the simulation, PEREGRINE records energy deposited at each interaction, which builds up a map of energy deposited in the transport mesh. After the Monte Carlo process is finished, a dose map is created by dividing the total energy deposited in each voxel by its material mass.

PEREGRINE transports photons through the body using the standard analog method [5]. Woodcock or delta-scattering [6] is used to efficiently track particles through the transport mesh. All photons below 0.1-keV energy are absorbed locally.

PEREGRINE transports electrons and positrons using a class II condensed-history scheme [7]. This procedure groups soft collisions with small energy losses or deflections, but simulates directly those major or catastrophic events in which the energy or

deflection angle is changed by more than a preset threshold. Delta-ray and bremsstrahlung production are modeled discretely for energy transfers  $> 200$  keV. PEREGRINE uses Moliere's theory of multiple elastic electron/positron scattering [8]. Pathlength corrections described in [9] are used to account for the effect of multiple scattering on the actual distance traveled by the electron or positron. A minimum electron/positron transport energy is assigned to each transport voxel based on range rejection. The range-rejection minimum energy corresponds to the minimum electron/positron range required to traverse 20% of the minimum zone dimension, with range determined as the minimum range calculated for that zone plus all directly adjacent zones. Two 511-keV photons are created at the end of each positron range. The direction of the first photon is chosen randomly, while the second is set to  $180^\circ$  opposed to the first.

### Physical Databases

The accuracy of Monte Carlo dose calculations depends on the availability of reliable, physically-consistent physical databases. For photon/electron/positron transport, PEREGRINE relies on the Lawrence Livermore National Laboratory Evaluated Physical Database, combined with stopping powers supplied by the National Institute of Standards and Technology.

### Photon Data

PEREGRINE accounts for photon interactions via the photoelectric effect, incoherent/coherent photon scattering, and pair production. All photon cross sections used by PEREGRINE are derived from the Lawrence Livermore National Laboratory Evaluated Photon Data Library (EPDL) [10]. EPDL data are taken from a variety of sources that have been selected for accuracy and consistency over a wide range of photon energies (10-eV–100-MeV) for all elements.

At low incident photon energies ( $< 0.1$  MeV for tissue components,  $< 1$  MeV for high-Z materials such as lead and tungsten), the photoelectric effect is the dominant absorption mechanism. The cross sections contained in PEREGRINE were obtained by direct evaluation of the relativistic S-matrix in a screened central potential [11]. These cross sections accurately describe ionization from electrons bound in isolated atoms and provide predictions at the percent level for compounds where the K and L shells are well-represented by atomic orbitals.

For most elements, at energies typical of those encountered for clinical photon beams, Compton scattering is the most important process in the photon-atom interaction. The Compton scattering cross sections used in PEREGRINE are obtained in the incoherent scattering factor approximation [12]. This approximation includes screening effects. Relativistic effects enter through use of the Klein-Nishina cross section.

Coherent scattering does not contribute significantly to the total photon-atom interaction cross section for most radiation therapy applications. However, these cross sections are still modeled, and were obtained under similar assumptions to those for incoherent scattering.

At very high incident photon energies ( $> 30$  MeV for tissue components,  $> 5$  MeV for high-Z materials such as lead and tungsten), the dominant photon interaction mechanism is pair production. The cross sections for pair and triplet production used by PEREGRINE include Coulomb and screening effects and radiative corrections [13].

### Electron/Positron Data

PEREGRINE accounts for the effects of large-angle elastic scattering (delta-ray production) and bremsstrahlung production on an event-by-event basis. All other energy-loss mechanisms are accounted for through continuous-slowing-down-approximation (CSDA) energy loss.

Moller (Bhabha) scattering is the ionization of an atom by an electron (positron). Moller and Bhabha cross sections and sampling methods follow those given in Messel and Crawford [14,15]. The threshold for these processes in PEREGRINE is set so that the ejected electron kinetic energy is  $> 200$  keV.

Bremsstrahlung cross sections contained in PEREGRINE are derived from the LLNL Evaluated Electron Data Library (EEDL) [16]. These cross sections were determined by Seltzer and Berger [17] by interpolating between the relativistic S-matrix data from the code of Tseng and Pratt [18] available up to 2 MeV, and the Bethe-Heitler result, expected to be valid above 50 MeV. Bremsstrahlung cross sections are processed to reflect a bremsstrahlung photon energy cutoff of 200 keV.

The radiative and collisional stopping powers used in PEREGRINE are described in [19]. During transport, PEREGRINE uses restricted collision and radiative stopping powers, which exclude energy lost due to Moller/Bhabha events with energy transfers  $> 200$  keV and bremsstrahlung events with energy transfers  $> 200$  keV. Restricted collision stopping powers are calculated as described in [20]. Restricted radiative stopping powers are calculated by subtracting the total energy transferred to the bremsstrahlung photon per distance, as determined from the bremsstrahlung cross section data.

## RESULTS

The accuracy of PEREGRINE transport calculations has been demonstrated by benchmarking PEREGRINE against a wide range of measurements and well-established Monte Carlo codes such as EGS4 and MCNP.

PEREGRINE benchmarks can be divided into two classes: the first set of comparisons validates the transport algorithms used to calculate dose in the patient; the second set of comparisons tests the accuracy of radiation source characterization and implementation, as well as transport through the patient. The second set is also useful for assessing the benefits of Monte Carlo calculations over current dose calculation algorithms.

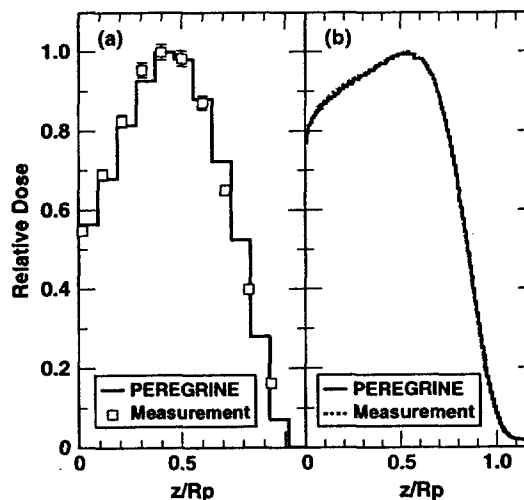


Figure 1. Comparison of PEREGRINE calculations with measurements for (a) a 1-MeV electron beam incident on carbon and for (b) a 22.5-MeV electron beam incident on water. Results are normalized to a relative maximum dose of 1.0. Distance is expressed in terms of practical range.

### Comparisons Using a Simple Radiation Source

We have compared PEREGRINE results with independent measurements and calculations for simple electron and photon sources. Figure 1(a) compares PEREGRINE depth dose calculations for a 1-MeV electron pencil beam incident normal on a

semi-infinite carbon slab with calorimeter measurements [21]. Figure 1(b) compares PEREGRINE depth dose calculations for a 22.5-MeV electron pencil beam incident on a water slab measurements [22]. Measurements were made for a broad beam with minimum scattering material, but with a correction for beam divergence. Calculations and measurements are normalized to maximum dose. Depths are given in fractions of the practical range. Calculations and measurements are in excellent agreement.

Figure 2 illustrates the results of comparing PEREGRINE calculations with EGS4 [23] for a 6-MV photon pencil beam incident normal to the center of a broad slab phantom. Figure 2(a) compares PEREGRINE and EGS4 calculations for water-air-water slabs; 2(b) compares results for water-iron-water slabs. EGS4 calculations were completed with bremsstrahlung photon (AP) and delta-ray production (AE) cutoff energies of 10 keV and 521 keV, respectively [22]. Results for both codes are in excellent agreement.

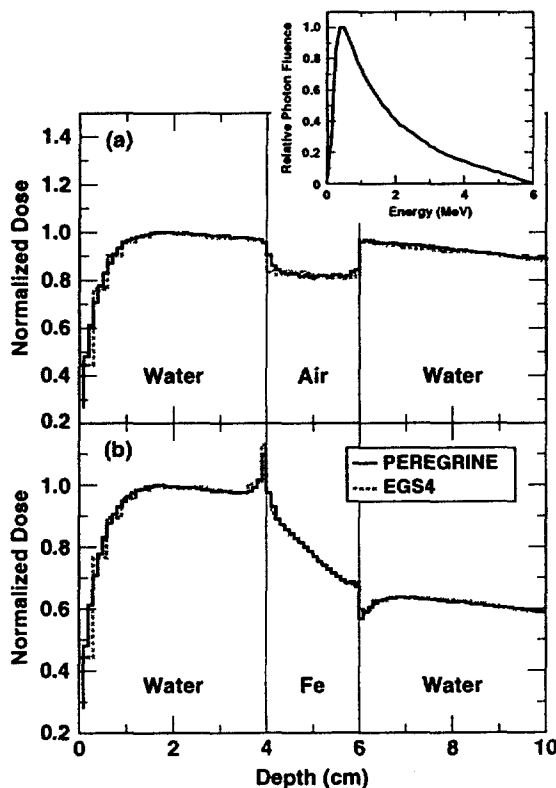


Figure 2. A 6-MV photon pencil beam incident on the center of a water-air-water (a) and on a water-iron-water phantom (b). The inset describes the photon energy spectrum used.

### Comparisons with Clinical Measurements

In addition to validating the accuracy of PEREGRINE Monte Carlo transport algorithms, we have also compared PEREGRINE calculations with a wide variety of clinical measurements for homogeneous and heterogeneous phantoms. Benchmarking against clinical measurements verifies the accuracy of radiation source characterization and implementation, as well as transport through the patient.

Figure 3 demonstrates the accuracy of PEREGRINE calculations for water phantom measurements made on a Varian 2100C 6-MV photon beam. We compare PEREGRINE dose calculations with ion chamber measurements [24] in a water phantom for  $2 \times 2$ ,  $10 \times 10$ , and  $20 \times 20$ -cm fields. Profile and depth dose comparisons are shown. Profiles are normalized to measured or calculated depth dose values for each depth. PEREGRINE calculations were completed using energy and angular distributions derived from a manufacturer-specified description of the Varian 2100C accelerator

head. The only free parameter in the accelerator source characterization was the electron spot size. These calculations were made with a version of PEREGRINE that included full photon transport in the collimator jaws. Ref. [1] shows similar comparisons for the version of PEREGRINE that assumes that all photons intersecting the collimator jaws are absorbed. Measurements were made using an air-equivalent ion chamber with an outer diameter of 6 mm, wall thickness of 0.4 mm, and active length of 3.3 mm. All measurements were smoothed.

Figure 4 illustrates the excellent agreement between PEREGRINE calculations and preliminary radiochromic film measurements for heterogeneous phantoms [24]. The phantom was irradiated at 100-cm SSD by a  $10 \times 10$ -cm beam. The solid water phantom had a 3-cm-wide-by-3-cm-thick square air heterogeneity (infinitely long on the gantry-target axis) centered along the central axis of the beam, with its top surface at 1.5-cm depth. The film was positioned perpendicular to the beam at 6-cm depth in the solid water phantom.

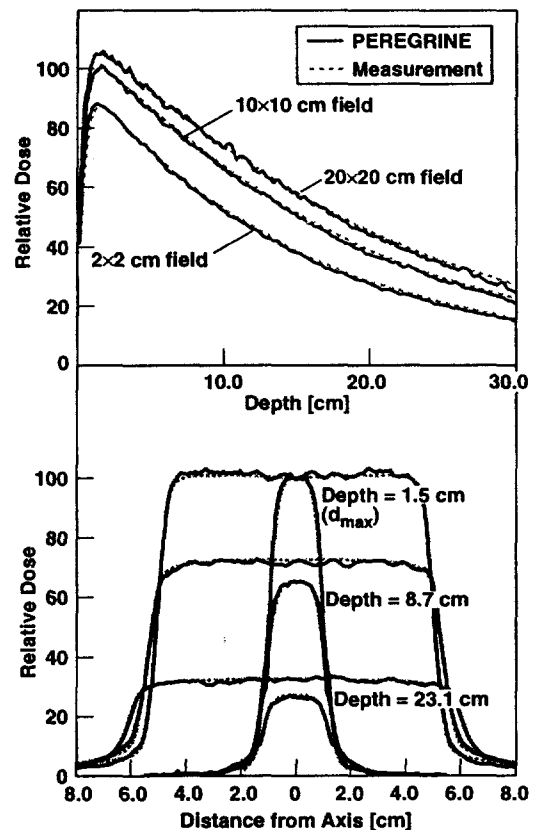


Figure 3. Comparison of PEREGRINE calculations with depth dose and profile ion chamber measurements in a water phantom for a Varian Clinac 2100C 6-MV photon beam.

### CLINICAL IMPLEMENTATION

The PEREGRINE Dose Calculation Engine (PDCE) combines the hardware, software, and networking components required to add this single-unit desktop design to any radiation treatment planning (RTP) system via a simple network connection, much like a file server.

The PDCE implements the PEREGRINE physics software under control of a modern, multithreaded operating system that supports the use of server-class, symmetric multiprocessing (SMP) microprocessors. The software design efficiently distributes the calculations for the problem so that dose is calculated by many microprocessors in parallel. The design is scaleable in a master-

slave configuration such that a number of slave main-boards can be configured to compute in parallel, while result accumulation and communications are controlled by a single master board.

The PDCE is constructed from off-the-shelf components originally developed for file- and Internet-server applications. The design combines a configurable number of motherboards interconnected by an internal high-speed network. Each main board supports up to four PentiumPro CPUs with supporting memory and peripherals. The use of commodity hardware and a flexible hardware architecture allows the engine to be configured at a number of cost/performance points. The design supports hardware upgrades for increased capability in microprocessor hardware technology.

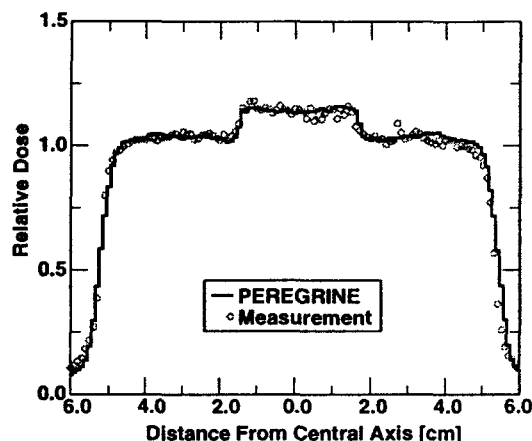


**Figure 4.** Comparison of PEREGRINE calculations with a radiochromic film profile measurement made at 6-cm depth in a solid water phantom with a  $3 \times 3$ -cm square air heterogeneity with its top surface at 1.5-cm depth. The radiation source was a Varian Clinac 2100C 6-MV  $10 \times 10$ -cm photon beam.

The PDCE can be optionally equipped with a display and supporting software to provide real-time visualization of the PEREGRINE Monte Carlo dose calculation while it computes. The display illustrates the effects of multiple beams and facilitates an early assessment of the plan's efficacy. Additional display capabilities are being developed to quantitatively monitor the progress of the dose calculation.

Once installed, PEREGRINE will operate as a dose calculation engine for a RTP system, calculating dose distributions for individual patient treatment plans. The RTP communicates with PEREGRINE via the AAPM Specifications for Treatment Planning Data Exchange [16], augmented by a small number of extensions, which provide additional beam- and patient-description data needed for Monte Carlo calculations. Once the treatment plan description is sent, the PDCE authenticates and checks files, computes the dose, and returns the results in new files for display and manipulation on the RTP system.

## SUMMARY

The PEREGRINE dose calculation system is designed to provide high resolution, high-accuracy dose calculations for clinical radiation therapy planning. PEREGRINE can be economically integrated into existing RTP systems as an "invisible" dose computer, providing state-of-the-art capability to all clinics. The availability of such calculations could improve effectiveness of

radiation therapy by providing accurate radiation treatment planning for every patient, facilitating accurate clinical trials and reliable implementation of these results throughout the medical community, providing accurate estimates of required doses for tumor control and normal tissue tolerance, and aiding in advancing the field of radiation oncology.

## REFERENCES

1. L. J. Cox, et al., 1997. This volume.
2. D. W. O. Rogers, et al., *Med. Phys.* **22** (5), 503–523 (1995).
3. J. F. Briesmeister, editor, *MCNP<sup>TM</sup> - A General Monte Carlo N-Particle Transport Code, Version 4A*, LA-12625, (Los Alamos National Laboratory, Los Alamos, NM, 1988).
4. A. E. Schach von Wittenau, et al., 1997. This volume.
5. L. L. Carter and E. D. Cashwell, *Particle-Transport Simulation with the Monte Carlo Method*, ERDA Critical Review Series, TID-26607, USERDA Distribution Category UC-34, (U.S. Energy Research and Development Administration, Oak Ridge, TN, 1975).
6. I. Lux and L. Koblinger, *Monte Carlo Particle Transport Methods: Neutron and Photon Calculations*, (CRC Press, Boca Raton, FL 1991), p. 222.
7. M. J. Berger, "Monte Carlo calculation of the penetration and diffusion of fast charged particles" In *Methods in Computational Physics, Volume I Statistical Physics*, edited by B. Alter, S. Fernbach, and M. Rotenberg (Academic Press, NY, 1963), p. 135.
8. H. A. Bethe, *Phys. Rev.* **89**, 1256 (1953).
9. A. F. Bielajew and D. W. O. Rogers, *NIM B* **18**, 165 (1987).
10. D. E. Cullen, et al., Report No. UCRL-50400 Vol. 6 Part B, Rev. 4 (Lawrence Livermore National Laboratory, Livermore, CA, 1989).
11. J. H. Scofield, Report No. UCRL-51326 (Lawrence Livermore National Laboratory, Livermore, CA, 1973).
12. Hubbell, et al., *J. Phys. Chem. Ref. Data* **4**, 471 (1975).
13. Hubbell, Gimm, and Overbo, *J. Phys. Chem. Ref. Data* **9**, 1023 (1980).
14. H. Messel and D. F. Crawford, *Electron-Photon Shower Distribution Function* (Pergamon Press, Oxford, UK, 1970).
15. W. R. Nelson, H. H. Hirayama, D. W. O. Rogers, *The EGS4 Code System*, SLAC-Report-265 (Stanford Linear Accelerator Center, Stanford, CA, 1985).
16. S. T. Perkins, D. E. Cullen, S. M. Seltzer, UCRL-50400 Vol. 31 (Lawrence Livermore National Laboratory, Livermore, CA, 1991).
17. S. Seltzer and M. J. Berger, *At. Data and Nucl. Data Tables* **35**, 345 (1985).
18. H. K. Tseng and R. H. Pratt, *Phys. Rev. Lett.* **33**, 516 (1974).
19. ICRU Report 37, *Stopping Powers for Electrons and Positrons* (ICRU Publications, Bethesda, MD, 1984).
20. K. R. Kase and W. R. Nelson, *Concepts of Radiation Dosimetry* (Pergamon Press, Oxford, UK, 1978).
21. G. J. Lockwood, et al., Sandia Report SAN79-0414 UC-34a (Sandia National Laboratories, Albuquerque, NM, 1985).
22. A. Brahme and H. Svensson, "Radiation beam characteristics of a 22 MeV microtron," *Acta Radiol. Oncol.* **18**, 244 (1979).
23. A. Bielajew (private communication).
24. K. A. Weaver and N. Albright (private communication).